Asymptotic approach to anti-plane dynamic problem of asymmetric three-layered composite plate

Rahmatullah Ibrahim Nuruddeen[1,2], R. Nawaz[1], Q. M. Zaigham Zia[1]

[1]Department of Mathematics, COMSATS University Islamabad, Park Road, Chak Shahzad, Islamabad 44000, Pakistan.

[2]Department of Mathematics, Faculty of Science, Federal University Dutse, Jigawa State, Nigeria.

Abstract

In this paper, the anti-plane shear motion of an asymmetric three-layered inhomogeneous elastic plate has been examined. An asymptotic approach is employed for the present investigation. Both the generalized and unified dispersion relations within the long-wave low-frequency range have been determined. The obtained unified dispersion relation is investigated taking into account the recently analyzed material contrast for layered plate with mixed stiff-soft layers of different material properties. Finally, we make comparison with symmetric plate being a special case of the asymmetric plate under consideration in the end.

Keywords:

1 Introduction

The mechanics of multilayered structures is gradually gaining ground due to its various applications in aerospace and automotive industries, glazing processes, electroplating and coating processes industrially, and metamaterials among others. The dynamics of multilayered elastic structures such as in plates, rods, beams and plane-wings has to do with vibrations or typical wave propagation in either the body or on the surface of the body, popularly known as Rayleigh waves, [1]. Many researchers have published quite a number of articles with regards to multilayered media including the thin walled elastics bodies [2], analysis of three-layered plate with thin soft core [3], parametric analysis of inhomogeneous periodic waveguides [4], long-wave asymptotic approximations in waveguides and periodic media [5], laminated composites and sandwiches [6-8] and the low-frequency approximations in symmetric three-layered plates [9-11]. Other similar studies include the low-frequency determination in multi-component elastic structure [12], asymptotic approach to plates with mixed boundary conditions [13], different investigations on five-layered plates [14-16]; see also [17-20] and the references therewith for related studies on elastic wave propagation among other.

However, in the present article, we extend the recent work by Prikazchikova et al. [10] on the low-frequency anti-plane shear dynamics of a three-layered symmetric inhomogeneous plate to the asymmetric three-layered version using the same asymptotic approach. The material contrast setup considered in [10] for a three-layered plate with stiff skin layers and soft core layer will be investigated here for the long-wave low-frequency dispersion. The paper is arranged as follows: section 2 gives the problem formulation, the determination of the dispersion relation and cut-off frequency is presented in section 3 for the generalized case and in section 4 for the unified case. We present the shortened dispersion relation for the unified case in section 5 and approximate equation of motion in section 6, and give the conclusion in section 7.

2 Problem Statement

Consider an anti-plane shear stress of an isotropic asymmetric three-layered strongly inhomogeneous plate with the the lower skin layer of thickness h_1, the core layer of thickness h_2 and the upper skin layer of thickness h_3 as shown in Fig. 1 below.

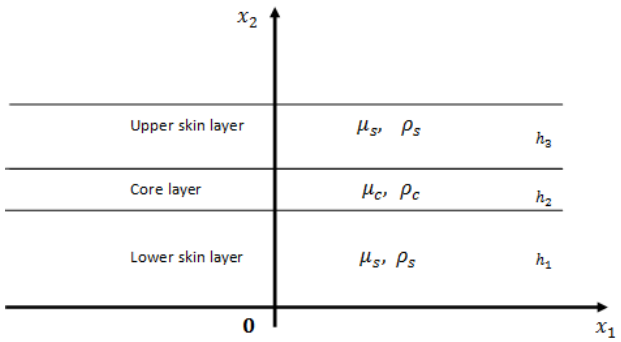

Fig. 1: Asymmetric three-layered plate.

We consider the anti-plane equation of motion in (x_1, x_2, t) given by

$$\frac{\partial \sigma_{13}^i}{\partial x_1} + \frac{\partial \sigma_{23}^i}{\partial x_2} = \rho_i \frac{\partial^2 U_i}{\partial t^2}, \quad i = sl, c, su, \tag{1}$$

where $x_n (n = 1, 2)$ are the spatial variables, t is the temporal variable, U_i the out of plane displacements for $i = sl$, $i = c$ and $i = su$ corresponding to the lower skin, core and the upper skin layers, respectively. The prescribed shear stresses $\sigma_{j3}^i, (j = 1, 2,)$ are defined by

$$\sigma_{j3}^i = \mu_i \frac{\partial U_i}{\partial x_j}, \ j = 1, 2, \tag{2}$$

where μ_i are the Lame's elastic constants of motion. More importantly, we remark here that both the lower and upper skin layers are considered to be of the same materials; thus, $\mu_{sl} = \mu_{su}$. We also consider the following interfacial continuity conditions of displacements and stresses:

$$\begin{aligned}
&\text{(a) } U_{\mathrm{c}}\left(x_1, x_2, t\right) = U_{\mathrm{sl}}\left(x_1, x_2, t\right), \text{ at } x_2 = h_1, \\
&\text{(b) } \sigma_{23}^c(x_1, x_2, t) = \sigma_{23}^{sl}(x_1, x_2, t), \text{ at } x_2 = h_1, \\
&\text{(c) } U_{\mathrm{c}}\left(x_1, x_2, t\right) = U_{su}\left(x_1, x_2, t\right), \text{at } x_2 = h_1 + h_2, \\
&\text{(d) } \sigma_{23}^c(x_1, x_2, t) = \sigma_{23}^{su}(x_1, x_2, t), \text{ at } x_2 = h_1 + h_2,
\end{aligned} \tag{3}$$

and the traction-free conditions on the skin faces as follows

$$\begin{aligned} &\text{(a) } \sigma_{23}^{sl}(x_1, x_2, t) = 0, \text{ at } x_2 = 0, \\ &\text{(e) } \sigma_{23}^{su}(x_1, x_2, t) = 0, \text{ at } x_2 = h_1 + h_2 + h_3. \end{aligned} \tag{4}$$

However in the present paper, we examine the anti-plane dynamic problem of an asymmetric three-layered inhomogeneous elastic composite plate that is made perfectly in contact between the layers coupled to the prescribed traction-free boundary conditions on the outer surfaces. The exact dispersion relation is to be investigated asymptotically within the zero cut-off frequency estimates in connection to the one of the material contrasting setups recently examined by Prikazchikova et al. [10] for a symmetric three-layered plate given by the following asymptotic relation [9]:

$$\mu \ll 1, \quad h \sim 1, \quad \rho \sim \mu, \tag{5}$$

corresponding to a plate with a soft core layer and stiff skin layers.

3 Generalized dispersion relation and cut-off frequency

In this section, we determine the generalized dispersion relation and cut-off frequency of the asymmetric problem under consideration given in Eqs. (1)-(4).

From Eqs. (1)-(2), we obtain the following classical wave equation

$$\frac{\partial^2 U_i}{\partial x_1^2} + \frac{\partial^2 U_i}{\partial x_2^2} = \frac{1}{c_i^2}\frac{\partial^2 U_i}{\partial t^2}, \quad i = sl,\ c,\ su, \tag{6}$$

where $c_i = \sqrt{\frac{\mu_i}{\rho_i}}$ are the shear transverse speeds in the respective layers of the plate. Further, with the harmonic solution assumption of the form

$$U_i(x_1, x_2, t) = u_i(x_2) e^{i(kx_1 - \omega t)},$$

we get the solutions of Eq. (6) in the the respective layers as follows:

$$u_i(x_2) = A_m \cosh\left(\sqrt{k^2 - \frac{\omega^2}{c_i^2}}\, x_2\right) + B_m \sinh\left(\sqrt{k^2 - \frac{\omega^2}{c_i^2}}\, x_2\right), \ i = sl,\ c,\ su, \tag{7}$$

where $m = 1, 2, 3$ are arbitrary constants in each layer to be determined from the prescribed conditions. Again ω and k in the above equation are the dimensional frequency and wave number, respectively. More, we obtain from Eq. (7) and the conditions given in Eqs. (3)-(4) the following generalized dispersion relation (see Appendix A for the dispersion matrix):

$$\alpha_1^2 \mu^2 \tanh(\alpha_1) + \alpha_2 \alpha_1 \mu \left(\tanh(\alpha_2 h) + \tanh(\alpha_2 l)\right) + \alpha_2^2 \tanh(\alpha_1) \tanh(\alpha_2 h) \tanh(\alpha_2 l) = 0, \tag{8}$$

where,

$$\alpha_1 = \sqrt{K^2 - \Omega^2},$$
$$\alpha_2 = \sqrt{K^2 - \frac{\mu}{\rho}\Omega^2}, \tag{9}$$

with the following dimensionless relations

$$\begin{aligned} \Omega =& \frac{\omega h_2}{c_c}, \qquad K = k h_2, \\ h =& \frac{h_1}{h_2}, \qquad l = \frac{h_3}{h_2}, \\ \rho =& \frac{\rho_c}{\rho_s}, \qquad \mu = \frac{\mu_c}{\mu_s}. \end{aligned} \tag{10}$$

The cut-off frequency is obtained from the generalized dispersion relation given in Eq. (8) at $K = 0$ as follows

$$\left(\sqrt{\mu\rho} - \tan(\Omega)\tan\left(h\sqrt{\frac{\mu}{\rho}}\Omega\right)\right)\tan\left(l\sqrt{\frac{\mu}{\rho}}\Omega\right) + \sqrt{\mu\rho}\tan\left(h\sqrt{\frac{\mu}{\rho}}\Omega\right) + \mu\rho\tan(\Omega) = 0. \tag{11}$$

The predicted single cut-off frequency from Eq. (11) is

$$\Omega \approx \sqrt{\frac{\rho(h+l+\rho)}{hl}} \ll 1, \tag{12}$$

with the low-frequency estimate provided

$$\frac{\rho r}{l} \ll h \ll \frac{l}{\mu r}, \tag{13}$$

where

$$r = h + l + \rho.$$

3.1 Generalized polynomial dispersion relation

The generalized polynomial dispersion relation is obtained from the exact generalized dispersion relation given in Eq. (8) via the Taylor's series expansion as follows:

$$\gamma_1 K^2 + \gamma_2 K^4 + \gamma_3 K^2\Omega^2 + \gamma_4\Omega^2 + \gamma_5\Omega^4 + \gamma_6 K^2\Omega^4 + \gamma_7 K^4\Omega^2 + ... = 0, \tag{14}$$

where

$$
\begin{aligned}
\gamma_1 =& 27h\mu + 27\mu^2 + 27l\mu, \\
\gamma_2 =& -9h^3\mu + 27hl - 9l^3\mu - 9\mu^2, \\
\gamma_3 =& \frac{18h^3\mu^2}{\rho} - \frac{54hl\mu}{\rho} + \frac{18l^3\mu^2}{\rho} + 18\mu^2, \\
\gamma_4 =& -\frac{27h\mu^2}{\rho} - 27\mu^2 - \frac{27l\mu^2}{\rho}, \\
\gamma_5 =& -\frac{9h^3\mu^3}{\rho^2} + \frac{27hl\mu^2}{\rho^2} - \frac{9l^3\mu^3}{\rho^2} - 9\mu^2, \\
\gamma_6 =& -\frac{27h^3l\mu^2}{\rho^2} - \frac{27hl^3\mu^2}{\rho^2} - \frac{9hl\mu^2}{\rho^2} - \frac{18hl\mu}{\rho}, \\
\gamma_7 =& \frac{27h^3l\mu}{\rho} + \frac{27hl^3\mu}{\rho} + \frac{18hl\mu}{\rho} + 9hl, \\
& \vdots
\end{aligned}
\tag{15}
$$

The first two modes from the generalized exact dispersion relation given in Eq. (8) are plotted in Fig. 2 for the non-estimated range and Fig. 3 for the estimated range of zero low-frequency, Eq. (13). The cut-off frequency is not noted in Fig. 2 owing to the selection of parameters outside Eq. (13); while it is noted in Fig. 3 with parameters within Eq. (13).

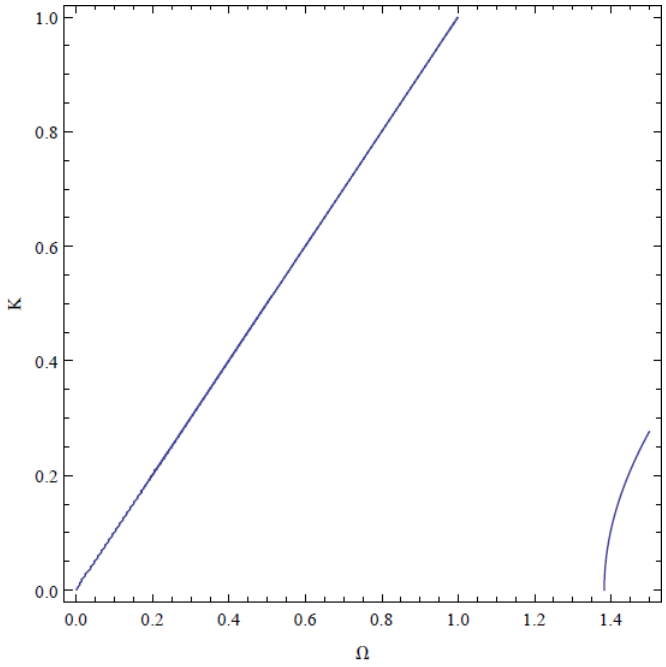

Fig. 2: The first two modes from Eq. (8) for the non-estimated range with $h = 1,\ \mu = 0.43,\ \rho = 2.21,\ l = 1.85.$

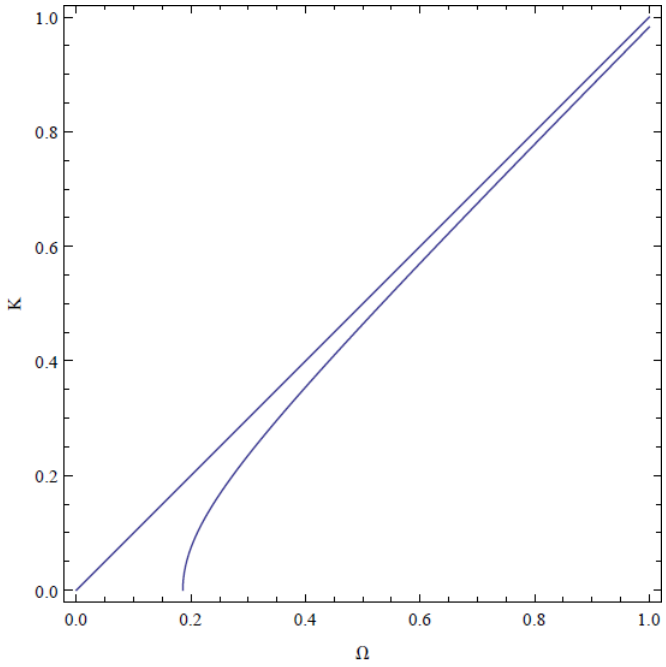

Fig. 3: The first two modes from Eq. (8) for the estimated range with $h = 1,\ \mu = 0.023,\ \rho = 0.023,\ l = 1.85.$

3.2 Generalized displacements and stresses

The displacements and stresses in the respective layers pf the plate are found while ignoring the exponential term as

The lower skin layer:

$$\begin{aligned} u_{sl} =& \frac{h_2}{\alpha_2}\cosh\left(\alpha_2 h \xi_{2_{\text{sl}}}\right), \\ \sigma_{13}^{sl} =& i\mu_s \frac{K}{\alpha_2}\cosh\left(\alpha_2 h \xi_{2_{\text{sl}}}\right), \\ \sigma_{23}^{sl} =& \mu_s \sinh\left(\alpha_2 h \xi_{2_{\text{sl}}}\right). \end{aligned} \tag{16}$$

The core layer:

$$\begin{aligned} u_c =& \frac{h_2}{\alpha_2}(\cosh\left(\alpha_2 h\right)\cosh\left(\alpha_1 \xi_{2_c}\right) + \nu \sinh\left(\alpha_2 h\right)\sinh\left(\alpha_1 \xi_{2_c}\right)), \\ \sigma_{13}^{c} =& i\mu_c \frac{K}{\alpha_2}(\cosh\left(\alpha_2 h\right)\cosh\left(\alpha_1 \xi_{2_c}\right) + \nu \sinh\left(\alpha_2 h\right)\sinh\left(\alpha_1 \xi_{2_c}\right)), \\ \sigma_{23}^{c} =& \mu_c \frac{\alpha_1}{\alpha_2}(\cosh\left(\alpha_2 h\right)\sinh\left(\alpha_1 \xi_{2_c}\right) + \nu \sinh\left(\alpha_2 h\right)\cosh\left(\alpha_1 \xi_{2_c}\right)). \end{aligned} \tag{17}$$

The upper skin layer:

$$\begin{aligned} u_{su} =& \frac{h_2}{\alpha_2}\lambda\left(\cosh\left(\alpha_2\left(h + l\xi_{2_{\text{su}}} + 1\right)\right) - \tanh\left(\alpha_2(h + l + 1)\right)\sinh\left(\alpha_2\left(h + l\xi_{2_{\text{su}}} + 1\right)\right)\right), \\ \sigma_{13}^{su} =& i\mu_s \frac{K}{\alpha_2}\lambda\left(\cosh\left(\alpha_2\left(h + l\xi_{2_{\text{su}}} + 1\right)\right) - \tanh\left(\alpha_2(h + l + 1)\right)\sinh\left(\alpha_2\left(h + l\xi_{2_{\text{su}}} + 1\right)\right)\right), \\ \sigma_{23}^{su} =& \mu_s\lambda\left(\sinh\left(\alpha_2\left(h + l\xi_{2_{\text{su}}} + 1\right)\right) - \tanh\left(\alpha_2(h + l + 1)\right)\cosh\left(\alpha_2\left(h + l\xi_{2_{\text{su}}} + 1\right)\right)\right). \end{aligned} \tag{18}$$

Where in Eqs.(17)-(18)

$$\begin{aligned} \lambda =& \text{sech}\left(\alpha_2 l\right)\cosh\left(\alpha_2(h + l + 1)\right)\left(\cosh\left(\alpha_1\right)\cosh\left(\alpha_2 h\right) + \nu \sinh\left(\alpha_1\right)\sinh\left(\alpha_2 h\right)\right), \\ \nu =& \frac{\alpha_2}{\alpha_1 \mu}, \end{aligned} \tag{19}$$

with the following scaled variables in Eqs. (16)-(18)

$$\begin{aligned} \xi_{2_{sl}} =& \frac{x_2}{h_1}, && 0 \le x_2 \le h_1, \\ \xi_{2_c} =& \frac{x_2 - h_1}{h_2}, && h_1 \le x_2 \le h_1 + h_2, \\ \xi_{2_{su}} =& \frac{x_2 - (h_1 + h_2)}{h_3}, && h_1 + h_2 \le x_2 \le h_1 + h_2 + h_3. \end{aligned} \tag{20}$$

4 Unified dispersion relation and cut-off frequency

In this section, we devise unification procedure to the generalized dispersion relation given in Eq. (8) owing to the presence of the two dimensionless thickness ratios in Eq. (10); that is, h and l, which ultimately prevents the contrast setup analysis given in Eq. (5). Thus, since the presence of these thickness ratios results in no analysis; we systematically relate the varying thicknesses of h_1 of the lower skin layer and h_3 of the upper skin layer as shown in Fig. 1 by the following relation $h_3 = \beta h_1$, for $\beta \in \mathbb{R}^+\backslash\{0,1\}$; the set of nonnegative real numbers excluding 0 and 1. We therefore obtain from Eq. (10) the following relation

$$l = \beta h, \quad \beta \in \mathbb{R}^+\backslash\{0,1\}. \tag{21}$$

It is remarkable here that $\beta \neq 0$ and $\beta \neq 1$. For if $\beta = 0$, the problem under consideration reduces to a two-layered plate problem; and if $\beta = 1$, the problem reduces to a symmetric three-layered inhomogeneous laminate which was recently analyzed by Prikazchikova et al. [10] for antisymmetric vibration mode.

With the present development, a unified dispersion relation is obtained from Eq. (11) as

$$\alpha_1^2\mu^2 \tanh(\alpha_1) + \alpha_2\alpha_1\mu \tanh(\alpha_2\beta h) + \alpha_2^2 \tanh(\alpha_1)\tanh(\alpha_2 h)\tanh(\alpha_2\beta h) + \alpha_2\alpha_1\mu \tanh(\alpha_2 h) = 0, \tag{22}$$

with Eqs. (9) and (10) holding but with $h_3 = \beta h_1$ as explained above. It is remarkable here that all the results in [10] can be recovered from the present work by simply setting $\beta = 1$. However, one should also note that both the symmetric modes and antisymmetric modes cases of the dispersion relations in connection to the symmetric three-layered plate are obtained by factorizing the dispersion relation given in Eq. (22) as posed by the asymmetric three-layered plate under consideration when $\beta = 1$.

The cut-off frequency from the unified dispersion relation given in Eq. (22) is given by

$$\left(\sqrt{\mu\rho} - \tan(\Omega)\tan\left(h\sqrt{\frac{\mu}{\rho}}\Omega\right)\right)\tan\left(\beta h\sqrt{\frac{\mu}{\rho}}\Omega\right) + \sqrt{\mu\rho}\tan\left(h\sqrt{\frac{\mu}{\rho}}\Omega\right) + \mu\rho\tan(\Omega) = 0. \tag{23}$$

The predicted single cut-off frequency from Eq. (11) is

$$\Omega \approx \sqrt{\frac{\rho(h+\beta h+\rho)}{\beta h^2}} \ll 1, \tag{24}$$

and over the global low-frequency inequalities

$$\begin{aligned} \Omega_1 &= \sqrt{\frac{\rho(h+\beta h+\rho)}{\beta h^2}} \ll 1, \\ \Omega_2 &= \sqrt{\frac{\mu(h+\beta h+\rho)}{\beta}} \ll 1. \end{aligned} \tag{25}$$

The first two modes from the unified exact dispersion relation given in Eq. (22) is plotted in Fig. 4 for the non-estimated range and Fig. 5 for the estimated range of zero cut-off frequencies, that is, within

the global frequency regime, Eq. (25). Additionally, the cut-off frequency is not noted in Fig. 4 owing to the selection of parameters outside Eq. (25); while the lowest low-frequency is noted in Fig. 5 with parameters within Eq. (25).

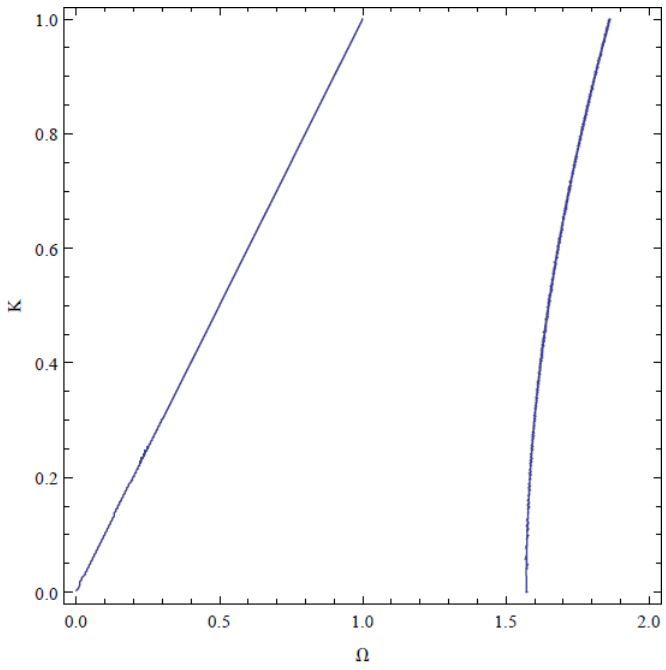

Fig. 4: The first two modes from Eq. (22) for the non-estimated range with $h = 1,\ \mu = 0.43,\ \rho = 2.21,\ \beta = 0.80.$

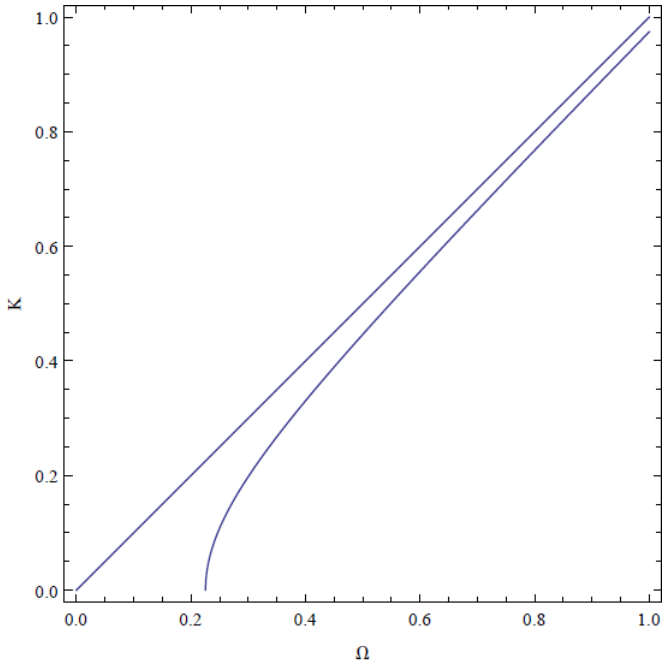

Fig. 5: The first two modes from Eq. (22) for the estimated range with $h = 1,\ \mu = 0.023,\ \rho = 0.023,\ \beta = 0.80.$

4.1 Unified polynomial dispersion relation

The unified polynomial dispersion relation is obtained from the exact unified dispersion relation given in Eq. (22) using the same Taylor's series expansion as follows:

$$\chi_1 K^2 + \chi_2 K^4 + \chi_3 K^2\Omega^2 + \chi_4 \Omega^2 + \chi_5 \Omega^4 + \chi_6 K^2\Omega^4 + \chi_7 K^4\Omega^2 + ... = 0, \tag{26}$$

where

$$
\begin{aligned}
\chi_1 =&27\beta h\mu + 27h\mu + 27\mu^2,\\
\chi_2 =&-9\beta^3h^3\mu - 9h^3\mu + 27\beta h^2 - 9\mu^2,\\
\chi_3 =&\frac{18\beta^3h^3\mu^2}{\rho} + \frac{18h^3\mu^2}{\rho} - \frac{54\beta h^2\mu}{\rho} + 18\mu^2,\\
\chi_4 =&-\frac{27\beta h\mu^2}{\rho} - \frac{27h\mu^2}{\rho} - 27\mu^2,\\
\chi_5 =&-\frac{9\beta^3h^3\mu^3}{\rho^2} - \frac{9h^3\mu^3}{\rho^2} + \frac{27\beta h^2\mu^2}{\rho^2} - 9\mu^2,\\
\chi_6 =&-\frac{27\beta^3h^4\mu^2}{\rho^2} - \frac{27\beta h^4\mu^2}{\rho^2} - \frac{9\beta h^2\mu^2}{\rho^2} - \frac{18\beta h^2\mu}{\rho},\\
\chi_7 =&\frac{27\beta^3h^4\mu}{\rho} + \frac{27\beta h^4\mu}{\rho} + \frac{18\beta h^2\mu}{\rho} + 9\beta h^2,\\
&\vdots
\end{aligned}
\tag{27}
$$

It is also remarkable here that having unified the varying dimensionless thicknesses h and l, we can now proceed with the investigation of the aforementioned contrast setup in connection to the formulated problem. Also it is worth noting here that, the generalized polynomial dispersion relation given in Eqs. (14)-(15) can be recovered from Eqs. (26)-(27) above upon substituting $\beta = \frac{l}{h}$.

4.2 Unified displacements and stresses

The shortened displacements and stresses in the respective layers are also determined as in above as follows

The lower skin layer:

$$
\begin{aligned}
u_{sl} =&\frac{h_2}{\alpha_2}\cosh\left(\alpha_2 h\xi_{2_{\mathrm{sl}}}\right),\\
\sigma_{13}^{sl} =&i\mu_s\frac{K}{\alpha_2}\cosh\left(\alpha_2 h\xi_{2_{\mathrm{sl}}}\right),\\
\sigma_{23}^{sl} =&\mu_s\sinh\left(\alpha_2 h\xi_{2_{\mathrm{sl}}}\right).
\end{aligned}
\tag{28}
$$

The core layer:

$$\begin{aligned}
u_c =& \frac{h_2}{\alpha_2}(\cosh(\alpha_2 h)\cosh(\alpha_1\xi_{2_c}) + \nu\sinh(\alpha_2 h)\sinh(\alpha_1\xi_{2_c})),\\
\sigma_{13}^c =& i\mu_c\frac{K}{\alpha_2}(\cosh(\alpha_2 h)\cosh(\alpha_1\xi_{2_c}) + \nu\sinh(\alpha_2 h)\sinh(\alpha_1\xi_{2_c})),\\
\sigma_{23}^c =& \mu_c\frac{\alpha_1}{\alpha_2}(\cosh(\alpha_2 h)\sinh(\alpha_1\xi_{2_c}) + \nu\sinh(\alpha_2 h)\cosh(\alpha_1\xi_{2_c})).
\end{aligned} \tag{29}$$

The upper skin layer:

$$\begin{aligned}
u_{su} =& \frac{h_2}{\alpha_2}\lambda\left(\cosh\left(\alpha_2\left(h+\beta h\xi_{2_{\mathrm{su}}}+1\right)\right) - \tanh\left(\alpha_2(h+\beta h+1)\right)\sinh\left(\alpha_2\left(h+\beta h\xi_{2_{\mathrm{su}}}+1\right)\right)\right),\\
\sigma_{13}^{su} =& i\mu_s\frac{K}{\alpha_2}\lambda\left(\cosh\left(\alpha_2\left(h+\beta h\xi_{2_{\mathrm{su}}}+1\right)\right) - \tanh\left(\alpha_2(h+\beta h+1)\right)\sinh\left(\alpha_2\left(h+\beta h\xi_{2_{\mathrm{su}}}+1\right)\right)\right),\\
\sigma_{23}^{su} =& \mu_s\lambda\left(\sinh\left(\alpha_2\left(h+\beta h\xi_{2_{\mathrm{su}}}+1\right)\right) - \tanh\left(\alpha_2(h+\beta h+1)\right)\cosh\left(\alpha_2\left(h+\beta h\xi_{2_{\mathrm{su}}}+1\right)\right)\right).
\end{aligned} \tag{30}$$

Where in Eqs.(29)-(30)

$$\begin{aligned}
\lambda =& \operatorname{sech}(\alpha_2\beta h)\cosh(\alpha_2(h+\beta h+1))\left(\cosh(\alpha_1)\cosh(\alpha_2 h) + \nu\sinh(\alpha_1)\sinh(\alpha_2 h)\right),\\
\nu =& \frac{\alpha_2}{\alpha_1\mu},
\end{aligned} \tag{31}$$

with the following scaled variables in Eqs. (28)-(30)

$$\begin{aligned}
\xi_{2_{sl}} =& \frac{x_2}{h_1}, && 0 \le x_2 \le h_1,\\
\xi_{2_c} =& \frac{x_2 - h_1}{h_2}, && h_1 \le x_2 \le h_1 + h_2,\\
\xi_{2_{su}} =& \frac{x_2 - (h_1+h_2)}{\beta h_1}, && h_1 + h_2 \le x_2 \le (1+\beta)h_1 + h_2.
\end{aligned} \tag{32}$$

4.3 Asymptotic formulae for unified displacements and stresses

To determine the asymptotic formulae for unified displacements and stresses presented in Eqs. (28)-(30); we make use of the normalised frequency and wave number of the form

$$K^2 = \mu K_*^2 \quad \text{and} \qquad \Omega^2 = \mu\Psi^2,$$

and obtain at the leading-order for the setup given in Eq. (5) as follows:

The lower skin layer:

$$\begin{aligned}
u_{sl} =& \frac{h_2}{\sqrt{\mu}\sqrt{K_*^2 - \Psi^2}},\\
\sigma_{13}^{sl} =& i\mu_s\frac{K_*}{\sqrt{K_*^2 - \Psi^2}},\\
\sigma_{23}^{sl} =& \mu_s\sqrt{\mu}\sqrt{K_*^2 - \Psi^2}\,\xi_{2_{\mathrm{sl}}}.
\end{aligned} \tag{33}$$

The core layer:

$$\begin{aligned} u_c =& \frac{h_2}{\sqrt{\mu}\sqrt{K_*^2-\Psi^2}}(1+(K_*^2-\Psi^2)\xi_{2_c}),\\ \sigma_{13}^c =& i\mu_c\frac{K_*}{\sqrt{K_*^2-\Psi^2}}(1+(K_*^2-\Psi^2)\xi_{2_c}),\\ \sigma_{23}^c =& \frac{\mu_c}{\sqrt{\mu}}\sqrt{K_*^2-\Psi^2}. \end{aligned} \tag{34}$$

The upper skin layer:

$$\begin{aligned} u_{su} =& \frac{h_2}{\sqrt{\mu}\sqrt{K_*^2-\Psi^2}}(1+K_*^2-\Psi^2),\\ \sigma_{13}^{su} =& i\mu_s\frac{K_*}{\sqrt{K_*^2-\Psi^2}}(1+K_*^2-\Psi^2),\\ \sigma_{23}^{su} =& \beta\mu_s\sqrt{\mu}\sqrt{K_*^2-\Psi^2}(1+K_*^2-\Psi^2)(\xi_{2_{\rm su}}-1). \end{aligned} \tag{35}$$

It is remarkable here that the following inference can be deduced for the present setup given in Eq. (5)

$$\begin{aligned} &\frac{\sigma_{13}^i}{\mu_i}\sim\frac{\sigma_{23}^i}{\beta\mu_i\sqrt{\mu}}\sim\frac{\sqrt{\mu}}{h_2}u_i, \qquad i=sl,\ su,\\ &\frac{\sigma_{13}^i}{\mu_i}\sim\frac{\sqrt{\mu}}{\mu_i}\sigma_{23}^i\sim\frac{\sqrt{\mu}}{h_2}u_i, \qquad i=c, \end{aligned} \tag{36}$$

where $\beta=1$ for $i=c,\ sl$ in the above equation; where sl and su stand for the lower skin and upper skin layers, respectively.

5 Shortened unified polynomial dispersion relations

In this section, we approximate the exact unified polynomial dispersion relation determined in Eq. (26) in relation to the contrasting setup earlier given in Eq. (5). However, since $\beta\in\mathbb{R}^+\backslash\{0,1\}$, it means that $\beta\in(0,1)\cup(1,\infty)$; which in relation to the asymmetric three-layered plate means that when $\beta\in(0,1)$ then the thickness of the lower skin layer is higher than that of the upper skin layer, and when $\beta\in(1,\infty)$ the reverse is the case. Thus, we consider β to be greater than one for convenience, say $\beta\in(1,3)$ to study the asymptotic behaviour in the present setup.

However, considering the setup given in Eq. (5) that describes a three-layered plate (asymmetric) with a core layer made of a soft material and the outer skin layers of hard or rather stiff material, from Eq. (26) the following asymptotic behaviour

$$\chi_1\sim\chi_4\sim\mu,\quad \chi_2\sim\chi_3\sim\chi_5\sim\beta\ \text{ and }\ \chi_6\sim\chi_7\sim\beta^3, \tag{37}$$

is deduced at the leading orders, where

$$\begin{aligned}
\chi_1 =&27\beta\mu + 27\mu^2 + 27\mu,\\
\chi_2 =&-9\beta^3\mu + 27\beta - 9\mu^2 - 9\mu,\\
\chi_3 =&18\beta^3\mu - 54\beta + 18\mu^2 + 18\mu,\\
\chi_4 =&-27\beta\mu - 27\mu^2 - 27\mu,\\
\chi_5 =&-9\beta^3\mu + 27\beta - 9\mu^2 - 9\mu,\\
\chi_6 =&-27\beta^3 - 54\beta,\\
\chi_7 =&27\beta^3 + 54\beta,\\
&\vdots
\end{aligned} \tag{38}$$

Thus, we obtain the shortened unified polynomial dispersion relation as follows

$$\chi_1 K^2 + \chi_2 K^4 + \chi_3 K^2\Omega^2 + \chi_4\Omega^2 + \chi_5\Omega^4 = 0, \tag{39}$$

where $\chi_j =$ for $j = 1, 3, 4, 5$ are given in Eq. (38). Thus, we give in Fig. 6 the first two modes for the exact (black solid line) and the shortened polynomial (dashed red line) dispersion relations (23) and (39) for the set of parameters $h = 1,\ \mu = 0.023,\ \rho = 0.023,\ \beta = 0.80$.

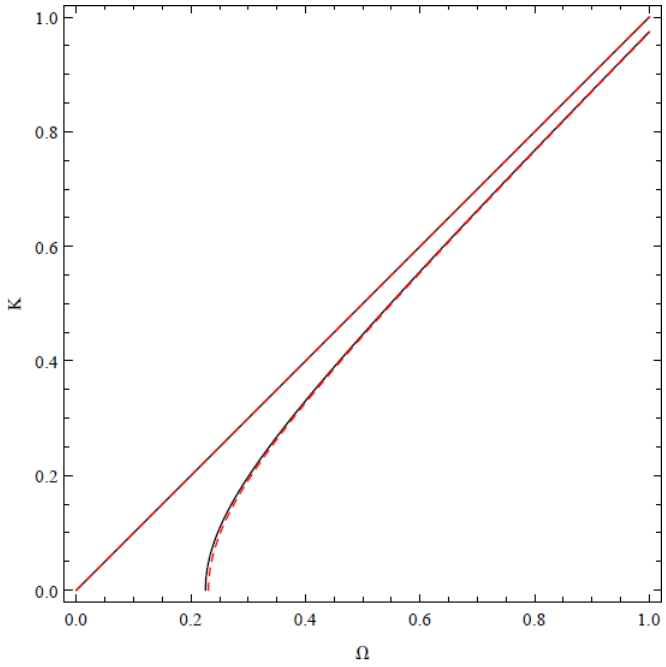

Fig. 6: The first two modes for the exact (black solid line) and shortened polynomial (dashed red line) dispersion relations Eq. (23) and Eq. (39).

6 Equations of motions approximations

In this section, we further ascertain the approximate unified equations of motion by incorporating the asymptotic material contrast given in Eq. (5). It is also worth mentioning here that we have utilised the upper skin layer as a basis of the computations in this section since the lower skin layer happened to be a special case of the upper one; revisit the preamble of Section 4.

More, to derive the approximate equations of motion, we make use of the following rescaling for x_1 and t variables as follows

$$x_1 = \frac{h_2}{\sqrt{\mu}}\xi_1, \qquad t = \frac{h_2}{c_{2_c}\sqrt{\mu}}\tau, \tag{40}$$

alongside the definitions given in Eq. (32) for x_2 coupled to the following normalized functions encouraged by Eq. (36)

$$\begin{aligned} u_i = \frac{h_2}{\sqrt{\mu}}w_i \quad \sigma^i_{13} = \mu_i\theta^i_{13}, \quad \sigma^i_{23} = \beta\mu_i\sqrt{\mu}\theta^i_{23}, \qquad i = sl,\ su, \\ u_i = \frac{h_2}{\sqrt{\mu}}w_i \quad \sigma^i_{13} = \mu_i\theta^i_{13}, \quad \sigma^i_{23} = \frac{\mu_i}{\sqrt{\mu}}\theta^i_{23}, \qquad i = c, \end{aligned} \tag{41}$$

with $\beta = 1$ for $i = sl$. Further, putting Eqs. (32), (40)-(41) into Eqs. (1)-(4) we get for the core and skin layers, respectively via Eq. (5) the following

$$\begin{aligned} &\mu\frac{\partial\theta^c_{13}}{\partial\xi_1} + \frac{\partial\theta^c_{23}}{\partial\xi_{2_c}} = \mu\frac{\partial^2 w_c}{\partial\tau^2}, \\ &\theta^c_{13} = \frac{\partial w_c}{\partial\xi_1}, \quad \theta^c_{23} = \frac{\partial w_c}{\partial\xi_{2_c}}, \end{aligned} \tag{42}$$

and

$$\begin{aligned} &\frac{\partial\theta^s_{13}}{\partial\xi_1} + \frac{\partial\theta^s_{23}}{\partial\xi_{2_s}} = \frac{\partial^2 w_s}{\partial\tau^2}, \\ &\theta^s_{13} = \frac{\partial w_s}{\partial\xi_1}, \quad \beta^2\mu\theta^s_{23} = \frac{\partial w_s}{\partial\xi_{2_s}}, \end{aligned} \tag{43}$$

for $s = sl, su$, with $\beta = 1$ for $i = sl$; and $h \sim 1 \sim \frac{\mu}{\rho}$. We also get the following continuity and boundary conditions

$$\begin{aligned} &w_c|_{\xi_{2_c}=0} = w_s|_{\xi_{2_{sl}}=1}, \\ &\theta^c_{23}|_{\xi_{2_c}=0} = \theta^s_{23}|_{\xi_{2_{sl}}=0}, \\ &\\ &w_c|_{\xi_{2_c}=1} = w_s|_{\xi_{2_{su}}=0}, \\ &\theta^c_{23}|_{\xi_{2_c}=1} = \theta^s_{23}|_{\xi_{2_{su}}=0}, \end{aligned} \tag{44}$$

and

$$\begin{aligned} &\theta^s_{23}|_{\xi_{2_{sl}}=0} = 0, \\ &\theta^s_{23}|_{\xi_{2_{su}}=1} = 0. \end{aligned} \tag{45}$$

We further adop the asymptotic series expansion in both the displacemets and stresses as follows

$$\begin{aligned} &w_i = w_{i,0} + \mu w_{i,1} + ..., \\ &\theta^i_{j3} = \theta^i_{j3,0} + \mu\theta^i_{j3,1} + ..., \quad i = c, s \quad j = 1, 2. \end{aligned} \tag{46}$$

Substituting Eq. (46) into Eqs. (42)-(45), we get at the leading order the following

$$\frac{\partial\theta^c_{23,0}}{\partial\xi_{2_c}} = 0, \quad \theta^c_{13,0} = \frac{\partial w_{c,0}}{\partial\xi_1}, \quad \theta^c_{23,0} = \frac{\partial w_{c,0}}{\partial\xi_{2_c}}, \tag{47}$$

and

$$\begin{aligned} &\frac{\partial\theta^s_{13,0}}{\partial\xi_1} + \frac{\partial\theta^s_{23,0}}{\partial\xi_{2_s}} = \frac{\partial^2 w_{s,0}}{\partial\tau^2}, \\ &\theta^s_{13,0} = \frac{\partial w_{s,0}}{\partial\xi_1}, \quad \frac{\partial w_{s,0}}{\partial\xi_{2_s}} = 0, \end{aligned} \tag{48}$$

together with the following continuity and boundary conditions

$$\begin{aligned} w_{c,0}|_{\xi_{2_c}=0} &= w_{s,0}|_{\xi_{2_{sl}}=1}, \\ \theta^c_{23,0}|_{\xi_{2_c}=0} &= \theta^s_{23,0}|_{\xi_{2_{sl}}=0}, \\ \\ w_{c,0}|_{\xi_{2_c}=1} &= w_{s,0}|_{\xi_{2_{su}}=0}, \\ \theta^c_{23,0}|_{\xi_{2_c}=1} &= \theta^s_{23,0}|_{\xi_{2_{su}}=0}, \end{aligned} \tag{49}$$

and

$$\begin{aligned} \theta^s_{23,0}|_{\xi_{2_{sl}}=0} &= 0, \\ \theta^s_{23,0}|_{\xi_{2_{su}}=1} &= 0. \end{aligned} \tag{50}$$

It is easy to obtain the following from Eq. (47) that

$$\theta^c_{23,0} = p(\xi_1, \tau), \qquad w_{c,0} = p(\xi_1, \tau)\xi_{2_c}, \qquad \theta^c_{13,0}\xi_{2_c}\frac{\partial p}{\partial \xi_1}, \tag{51}$$

and from Eq. (48)

$$w_{s,0} = p(\xi_1, \tau), \qquad \theta^s_{13,0} = \xi_{2_c}\frac{\partial p}{\partial \xi_1}, \qquad \theta^s_{23,0} = \left(\frac{\partial^2 p}{\partial \tau^2} - \frac{\partial^2 p}{\partial \xi_1^2}\right)\xi_{2_s}, \tag{52}$$

with $\theta^s_{23,0}$ in Eq. (52) suitably constructed. However, the missing of the constant parameter β in Eq. (52) prompts us to move to the next asymptotic order which gives

$$\begin{aligned} \frac{\partial \theta^s_{13,1}}{\partial \xi_1} + \frac{\partial \theta^s_{23,1}}{\partial \xi_{2_s}} &= \frac{\partial^2 w_{s,1}}{\partial \tau^2}, \\ \theta^s_{13,1} = \frac{\partial w_{s,1}}{\partial \xi_1}, \quad \beta^2 \theta^s_{23,0} &= \frac{\partial w_{s,1}}{\partial \xi_{2_s}}, \end{aligned} \tag{53}$$

with the continuity and boundary conditions

$$\begin{aligned} w_{c,1}|_{\xi_{2_c}=0} &= w_{s,1}|_{\xi_{2_{sl}}=1}, \\ \theta^c_{23,1}|_{\xi_{2_c}=0} &= \theta^s_{23,1}|_{\xi_{2_{sl}}=0}, \\ \\ w_{c,1}|_{\xi_{2_c}=1} &= w_{s,1}|_{\xi_{2_{su}}=0}, \\ \theta^c_{23,1}|_{\xi_{2_c}=1} &= \theta^s_{23,1}|_{\xi_{2_{su}}=0}, \end{aligned} \tag{54}$$

and

$$\begin{aligned} \theta^s_{23,1}|_{\xi_{2_{sl}}=0} &= 0, \\ \theta^s_{23,1}|_{\xi_{2_{su}}=1} &= 0. \end{aligned} \tag{55}$$

Therefore with the help of $\theta^s_{23,0}$ from Eq. (52), we get the following relations

$$w_{s,1} = \beta^2\left(\frac{\partial^2 p}{\partial \tau^2} - \frac{\partial^2 p}{\partial \xi_1^2}\right), \quad \theta^s_{13,1} = \beta^2\left(\frac{\partial^3 p}{\partial \xi_1 \partial \tau^2} - \frac{\partial^3 p}{\partial \xi_1^3}\right), \quad \theta^s_{23,1} = 3\left(\frac{\partial^2 p}{\partial \tau^2} - \frac{\partial^2 p}{\partial \xi_1^2}\right)\xi_{2_s}, \tag{56}$$

which from Eq. (53) (first line) satisfies the following equation

$$\frac{1}{3}\left(\frac{\partial^4 p}{\partial \xi_1^4} - 2\frac{\partial^4 p}{\partial \xi_1^2 \partial \tau^2} + \frac{\partial^4 p}{\partial \tau^4}\right) - \frac{1}{\beta^2}\left(\frac{\partial^2 p}{\partial \tau^2} - \frac{\partial^2 p}{\partial \xi_1^2}\right) = 0. \tag{57}$$

Expressing Eq. (57) using the skin displacement notation, being $u_s(x_1, t) \approx p(\xi_1, \tau)$, we get

$$\frac{1}{3}\left(\frac{\partial^4 u_s}{x_1^4} - 2\frac{\partial^4 u_s}{\partial x_1^2 \partial t^2} + \frac{\partial^4 u_s}{\partial t^4}\right) - \frac{1}{\beta^2}\left(\frac{\partial^2 u_s}{\partial t^2} - \frac{\partial^2 u_s}{\partial x_1^2}\right) = 0. \tag{58}$$

Now with the help of the formula $u_s = e^{i(kx_1 - \omega t)}$, we get from Eq. (58) the following dispersion relation

$$\frac{1}{\beta^2}k^2 - \frac{1}{3}k^4 + \frac{2}{3}k^2\omega^2 - \frac{1}{\beta^2}\omega^2 - \frac{1}{3}\omega^4 = 0, \tag{59}$$

which indeed coincides with Eq. (39) at the higher-order terms of β in $\chi_j (j = 1, 2, ..., 5)$.

7 Conclusion

In this paper, the anti-plane dynamic problem of an asymmetric three-layered inhomogeneous elastic plate has been investigated successfully via the asymptotic approach. The asymmetric layered plate considered is made perfectly in contact between the three layers, while traction-free boundary conditions are prescribed on the outer surfaces. Furthermore, due to the varying lengths of the outer layers, a new parameter β is introduced to relate the two lengths and thus make it possible for the material contrast investigation. The long-wave low-frequency generalized and unified dispersion relations have been determined and examined via the polynomial dispersion relation in connection to the recently analyzed material contrast for a plate with mixed stiff-soft layers of different material properties in the composites. In comparison with setup (a) of the symmetric three-layered plate [10], the present study also shows that the obtained dispersion relation is valid over the whole cut-off frequency range as depicted in figure 6. However, approximate equations of motion obtained in the case of symmetric three-layered plate are better than those of the asymmetric case in the sense of simplicity. We finally recommend that an extension in the contrast setups be made to be able to analyze such problems with more than one dimensionless parameters in μ, h, and ρ directly without the proposed unification. Also, the corresponding inverse problem of the formulated problem will be an interesting one.

Acknowledgment

The first author, Rahmatullah Ibrahim Nuruddeen sincerely acknowledges the 2017 CIIT-TWAS Full-time Postgraduate Fellowship Award (FR Number: 3240299480).

Data Availability

All the data used for the numerical simulations and comparison purpose have been reported and visualized in the graphical illustrations and nothing is left.

Conflict of interests

On behalf of all authors, the corresponding author states that there is no conflict of interests.

Appendix A

The 5×5 dispersion matrix generated by the problem in Section 3 is given here as:

$$\begin{pmatrix} \cosh(p_1 R_s) & \sinh(p_1 R_s) & -\cosh(p_1 R_c) & -\sinh(p_1 R_c) & 0 \\ 0 & 0 & \cosh(h_1 R_c) & \sinh(h_1 R_c) & -\cosh(h_1 R_s) \\ \sinh(p_1 R_s) & \cosh(p_1 R_s) & -q\sinh(p_1 R_c) & -q\cosh(p_1 R_c) & 0 \\ 0 & 0 & q\sinh(h_1 R_c) & q\cosh(h_1 R_c) & -\sinh(h_1 R_s) \\ \sinh(p_2 R_s) & \cosh(p_2 R_s) & 0 & 0 & 0 \end{pmatrix},$$

with the following shortend terms

$$p_1 = h_1 + h_2,\ p_2 = h_1 + h_2 + h_3,\quad q = \frac{R_c \mu_c}{R_s \mu_s},\quad R_s = \sqrt{k^2 - \frac{\omega^2}{c_s^2}},\quad R_{\mathrm{c}} = \sqrt{k^2 - \frac{\omega^2}{c_{\mathrm{c}}^2}}.$$

References

[1] Achenbach, J. D., Wave Propagation in Elastic solids, Eight impression, Elsevier, Netherland, 1999.

[2] Kaplunov, J.D., Kossovich, L.Y., Nolde, E.V., Dynamics of Thin Walled Elastic Bodies, San Diego, CA: Academic Press, 1998.

[3] Altenbach, H., Eremeyev, V.A., and Naumenko, K., On the use of the first order shear deformation plate theory for the analysis of three-layer plates with thin soft core layer, ZAMM, 95(10), 1004-1011, 2015.

[4] Kaplunov, J., Nobili, A., Multi-parametric analysis of strongly inhomogeneous periodic waveguides with internal cut-off frequencies, Math. Methods Appl. Sci., 40(9), 3381-3392, 2017.

[5] Craster, R., Joseph, L., Kaplunov, J., Long-wave asymptotic theories: the connection between functionally graded waveguides and periodic media, Wave Motion, 51(4), 581-588, 2014.

[6] Sayyad, A. S, Ghugal, Y. M., Bending, buckling and free vibration of laminated composite and sandwich beams: a critical review of literature. Compos. Struct. 171, 486504, 2017.

[7] Naumenko, K., Eremeyev, V. A., A layer-wise theory for laminated glass and photovoltaic panels. Compos. Struct., 112, 283291, 2014.

[8] P. Lee, N. Chang., Harmonic waves in elastic sandwich plates, J. Elasticity, 9(1), 51-69, 1979.

[9] Kaplunov, J., Prikazchikov, D., Prikazchikova, L., Dispersion of elastic waves in a strongly inhomogeneous three-layered plate, Int. J. Solids Struct., 113: 169179, 2017.

[10] Prikazchikov, L.A., Aydn, Y.E., Erba, B., Kaplunov, J., Asymptotic analysis of anti-plane dynamic problem for a three-layered strongly inhomogeneous laminate, Math. Mechanics Solids, 2018.

[11] Erbas, B., Low frequency antiplane shear vibrations of a three-layered elastic plate, Eskiehir Techn. University J. Sci. Techno., A- Appl. Sci. Eng., 19(4), 867 - 879, 2018.

[12] Kaplunov, J., Prikazchikov, D.A., Prikazchikov, L.A., Sergushova, O., The lowest vibration spectra of multi-component structures with contrast material properties. J Sound Vib., 445, 132-147 (2019).

[13] Andrianov, I.V., Awrejcewicz, J., Danishevs'kyy, V.V., Ivankov, O.A.,Asymtotic Methods in the Theory of Plates with Mixed Boundary Conditions, John Wiley & Sons, Ltd. United Kingdom, 2014.

[14] Nuruddeen, R.I., Nawaz, R, Zia, Z.Q.M., Asymptotic analysis of an anti-plane shear dispersion of an elastic five-layered structure amidst contrasting properties, Arch. Appl. Mech., 2020. DOI: 10.1007/s00419-020-01702-6

[15] Lpez-Aenlle, M., Pelayo, F., Static and dynamic effective thickness in five-layered glass plates, Solids Struct., 212(15), 259-270, 2019.

[16] Shishehsaz, M. Raissi, H., Moradi, S., Stress distribution in a five-layer circular sandwich composite plate based on the third and hyperbolic shear deformation theories, Mechanics Adv. Materials Struct., 2019.

[17] Reut, V., Vaysfeld, N., Zhuravlova, Z., Elastic crack-tip stress field in a semi-strip, Frattura ed Integrit Strutturale, 44, 82-93, 2018.

[18] Demirkus, D., Antisymmetric bright solitary SH waves in a nonlinear heterogeneous plate, Z. Angew. Math. Phys. 69, 128, 2018.

[19] Nuruddeen, R.I., Nawaz, R, Zia, Z.Q.M., Investigating the viscous damping effects on the propagation of Rayleigh waves in a three-layered inhomogeneous plate, Physica Scripta, 2020.

[20] Nawaz, R., Ayub, M., Closed form solution of electromagnetic wave diffraction problem in a homogeneous bi-isotropic medium, Math. Meth. Appl. Sci., 2015.